JOURNAL OF MATERIALS SCIENCE: MATERIALS IN MEDICINE 9 (1998) 603–609

Fibrous wound repair associated with biodegradable poly-*L*/*D*-lactide copolymer implants: study of the expression of tenascin and cellular fibronectin

R. KONTIO*, A. SALO, R. SUURONEN, C. LINDQVIST
Department of Maxillofacial Surgery, Helsinki University Central Hospital, Kasarminkatu 11-13, 00130 Helsinki, Finland

J. H. MEURMAN
Faculty of Dentistry, University of Kuopio, Finland

I. VIRTANEN
Institute of Biomedicine, Department of Anatomy, Helsinki University, Helsinki, Finland
E-mail: risto.kontio@medius.inet.fi

Extracellular matrix (ECM) proteins are known to play a role in inflammatory and hyperplastic processes. Our aim in the present study was to study the distribution of tenascin (Tn), cellular fibronectins (cFn) and myofibroblasts around biodegradable poly-*L*/*D*-lactide (PLA) implants with monoclonal antibodies (MAb). Ethylene-oxide and gamma-irradiation sterilized PLA plate-type implants were inserted into the dorsal subcutaneous tissue of ten adult rabbits. Follow-up times were 4, 12, 16, 36 and 48 wk. Only some inflammatory cells were observed. In electron microscopy, a close coherence between the implant and the stromal tissue was seen. Immunoreactivity for Tn, cFn and α-actin was detected as a distinct layer bordering the implant, regardless of the sterilization method for the first 36 wk. From week 36 onwards, Tn immunoreactivity was downregulated while cFn immunoreactivity still persisted. A moderate upregulation for myofibroblasts was seen on the week 48 specimens, when hydrolysation of PLA implant had started. The persistent content of myofibroblasts, Tn and cFn suggests a prolonged wound healing produced by PLA implants. The absence of Tn at the week 48 specimens suggests that cFn, rather than Tn may be needed for α-actin-mediated contraction by myofibroblasts.

1. Introduction

When the biodegradable materials for fracture and reconstructive surgery were introduced, it was hypothesized that this would start a new era in bone fixation [1, 2]. Indeed, biodegradable polylactide (PLA) implants have recently been successfully applied for internal fixation of bone fractures, but at the same time abacterial inflammatory reactions have been noted [3, 4]. In recently published data, a foreign body-type reaction has also been shown to occur [5].

Extracellular matrix (ECM) proteins are known to play a role in normal histodifferentation and as well as in regenerative and reparative processes [6]. Wound healing induces a complex connective tissue response, including synthesis and deposition of ECM glycoproteins tenascin (Tn) and cellular fibronectins (cFns), otherwise seen during embryonic development, re-expressing during allograft rejection and in malignancy [7–9]. Inflammation and wound healing are regulated by adhesive intercellular and cell-to-ECM interactions, in which both cFns and Tn play a role, with opposite functions [10, 11].

The wound contraction phenomenon is generally attributed to myofibroblasts found in granulation tissue. This may withstand several weeks [12]. During the wound healing process, these cells produce Tn and cFn, which both provide trophic support in the connective tissue by paracrine and autocrine mechanisms [6].

We were prompted to evaluate the tissue distribution of Tn, locally produced cFn and myofibroblasts around PLA implants. These two ECM proteins were chosen because of their partially opposite functions and their documented restricted and scheduled expression during wound healing and repair [11].

*Author to whom all correspondence should be addressed.

0957–4530

2. Material and methods

2.1. Implant material

The biodegradable implants were manufactured of poly-*L*/*D*-lactic acid stereocopolymer with *L*-lactide/*D*-lactide molar ratio of 85/15. The raw material was obtained from PURAC biochem b.v. (Gorinchem, The Netherlands). The specific details of the raw polymer, as given in the manufacturer's certificate of analysis, were as follows: intrinsic viscosity 3.6 dl g^{-1} (in chloroform at 25 °C), weight average molecular weight 510 kDa (according to gas phase chromatography analysis), specific optical rotation $-114°$ (in chloroform at 25 °C), glass-transition temperature 59 °C (according to differential scanning calorimetry measurement). The polymer was melt extruded at 135 °C into circular rods of diameter 5 mm using Axon BX-15 extruder (Axon, Sweden) which were subsequently drawn at 90 °C through a heated conical die to a draw ratio of 2.5. The drawn rods of diameter 3.8 mm and length of 60 mm were compressed between flat metal surfaces at 115 °C using 100 kN compression force to plates of thickness 0.3 mm. The plates were cut to the width of 12 mm and to the length of 50 mm and the mid portion was perforated (length of perforated portion 9 mm, hole diameter 1.5 mm, distance between holes 3 mm, and total number of holes 18 in four rows). The plates were sterilized, either with 2.5 MRad dose of gamma-irradiation (g.i.) or ethylene oxide (e.o.).

2.2. Experimental protocol

A total number of 60 poly-*L*/*D*-lactic acid stereocopolymer (PLA) e.o. and g.i. plates were inserted into the dorsal subcutaneous tissue of 10 adult rabbits; two rabbits served as controls. The animals were anaesthetized with subcutaneous (s.c.) ketamine (Ketalar®, Parke-Davis, Barcelona, Spain) 25 mg kg^{-1} and medetomiden (Domitor®, Lääke-Farmos, Turku, Finland) 0.3 mg kg^{-1}. Preoperatively, 70 000 IU kg^{-1} sodium benzylpenicillin (Geepenil®, Orion, Espoo, Finland) was given s.c. for infection prophylactics. The skin incision was closed in one layer by Dermalone® 3-0 sutures. The control rabbits were operated in the same manner but without PLA implantation. The rabbits were sacrificed after follow-up of 4, 12, 16, 36 and 48 wk. The follow-up groups consisted of two animals. The plates and surrounding connective tissues were identified and carefully removed. The control animals were sacrificed after 4 wk and the connective tissue near to the incision was removed.

2.3. Immunofluorescence microscopy

Connective tissue collars enveloping the plates were removed and cut into halves. One half was tied into 10% formalin solution for the haematoxylin–eosin staining. The other half was snap-frozen in liquid nitrogen and stored at −80 °C for immunohistochemistry. Cryosections 5 μm thick were cut, air-dried and briefly fixed in cold (−20 °C) acetone. Indirect immunofluorescence microscopy was performed by using MAb 100EB2 [13] against human Tn, MAb 52DH1 [14] against human extradomain A cFn, and MAb against smooth muscle α-actin (Sigma, St Louis, MO, USA). The specimens were incubated with the MAbs for 30 min. Fluorescein isothiocyanate (FITC)-coupled sheep anti-mouse IgG antiserum (dilution 1/120, Sigma, St Louis, MO, USA) was then applied. The sections were coated with glycerine (dilution 3/1 with phosphate buffered saline). The sections were examined in a Leica Aristoplan microscope equipped with appropriate filters.

The degree of immunofluorescence staining was evaluated by two observers independently using ×100 to ×200 magnification by means of an arbitrary scale (− = non or slight reactivity, + = moderate or high reactivity). As controls, the 4 wk specimens were used for evaluating the specificity of the immunochemical reactions.

2.4. Electron microscopy

For electron microscopy, a small fragment of connective tissue was cut. These fragments were fixed in 2% glutaraldehyde in phosphate-buffer (0.1 M, pH 7.4) for 60 min and postfixed in 1% osmium tetroxide in the same buffer. After dehydration in graded series of ethanol and acetone, the specimens were embedded in Epon 812. Thin sections (1 μm) were cut and stained with methyl blue and studied under a stereomicroscope for orientation. Ultra-thin sections were then made of representative specimens stained with uranyl acetate and lead citrate and the sections were studied in a Jeol 1200EX transmission electron microscope operating at 60 kV accelerating voltage.

2.5. Strength measurements and *in vitro* studies

The tensile strengths of the intact plates and after *in vitro* exposure were measured using a Lloyd 6000R Materials Testing Machine (Lloyd Instruments PLC, Fareham, UK) at room temperature (22–23 °C). Triplicate samples were tested at each follow-up time. The measurements were performed on wet samples because drying of the incubated plates leads to a decrease of their strength. The cross-head speed was 10 mm and gauge length 20 mm.

The PLA plates were immersed in (2.87 g l^{-1}) Na_2HPO_4–(0.67 g l^{-1}) NaH_2PO_4 buffered saline (NaCl 5.9 g l^{-1}) at pH 7.4 and 0.127 M, and held at 37 °C. Samples were removed from the solution at 1, 2, 3, 4, 8, 12, 16 and 26 wk and changes in tensile strength and crystallinity, as well as changes in intrinsic viscosity (indicative of molecular weight) were determined.

2.6. Thermal analysis and molecular weight measurements

A Perkin–Elmer DSC-7 differential scanning calorimeter (DSC, Perkin–Elmer Co., USA), calibrated with indium standards, was used to determine the heat of fusion of intact PLA plates and after *in vitro* and *in vivo* exposure. The DSC was operated at a heating rate of 20 °C min^{-1}. Dry 6 ± 1 mg samples evacuated at

room temperature for 3 d were used in each case. The samples were heated in a nitrogen atmosphere from room temperature to 200 °C and the heat of fusion was estimated from the area enclosed by the DSC curve and the baseline. The level of crystallinity was estimated from the heat of fusion, assuming $93.7\,J\,g^{-1}$ calculated by Fischer *et al.* [15] for perfectly crystalline PLLA. Duplicate samples were used in each case.

The solution viscosities (according to ASTM D 445-88) of the plates were measured in chloroform at 25 °C with an Ubbelohde capillary viscometer (type 0a according to ASTM D 446). Inherent viscosities (η in $dl\,g^{-1}$) in a 0.1% ($0.1\,g\,dl^{-1}$) solution were determined as an indication of molecular weight decrease during degradation [16]. Viscosity-average molecular weights ($g\,mol^{-1}$) were estimated using the Mark-Houwink equation and the parameters $k = 2.21 \times 10^{-4}$ and $a = 0.77$ [17].

3. Results

3.1. Microscopic findings

In light microscopy, all the implants were enveloped by a connective tissue collar, consisting mainly of fibroblast-like cells. Some macrophages, lymphocytes and polymorphonuclear leukocytes were observed, suggesting a low-grade chronic inflammation. From 16 wk onwards, the expression of inflammatory cells was low. The PLA implant and connective tissue interface was tight (Fig. 1a and b). On 36 and 48 wk specimens, pseudosynovial membrane-like tissue interfacing PLA implants was detected. No differences between g.i. or e.o. sterilization were discovered. Specimens at 48 wk showed minor upregulation of inflammatory cells and moderate upregulation of myofibroblasts, at the same time as macroscopically hydrolysation of PLA material was seen to commence (Fig. 1c). In the electron microscopy specimens, occasionally a layer of amorphous-appearing material was found to surround the PLA material while the cell-to-PLA contact was tight in most cases observed (Fig. 2a and b).

During the first 36 wk, there was an intense immunofluorescence for both Tn and cFn around implant material. Immunoreactivities for both Tn and cFn were detected as a highly fluorescent, but restricted layer close to the implant (Fig. 3a–f). MAb against smooth muscle α-actin demonstrated a thick layer of activated myofibroblasts adjacent to the implant in areas presenting Fn- and Tn-immunoreactivities (not shown). From week 36 onwards, Tn immunoreactivity was promptly downregulated and could not be traced on the 48 wk specimen (Fig. 4a). An intense immunoreactivity for cFn, however, persisted to the end of the study (Fig. 4b). At 48 wk, an intense immunoreactivity for smooth muscle α-actin was still seen around the implant material (Fig. 4c).

3.2. Mechanical study

Mechanically the PLA implant was inadequate; plate form implants were already broken *in vivo* at week 4. At 48 wk, the g.i. implants had macroscopically disappeared and the e.o. implants were detected as rounded masses.

In vitro tensile strengths are presented in Table I. The initial tensile strength was 43.8 MPa for e.o. and

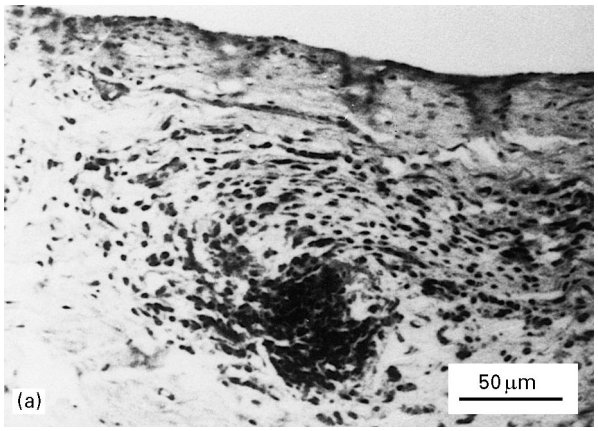

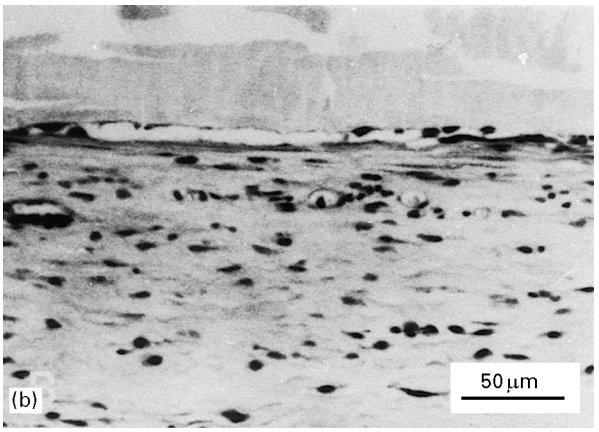

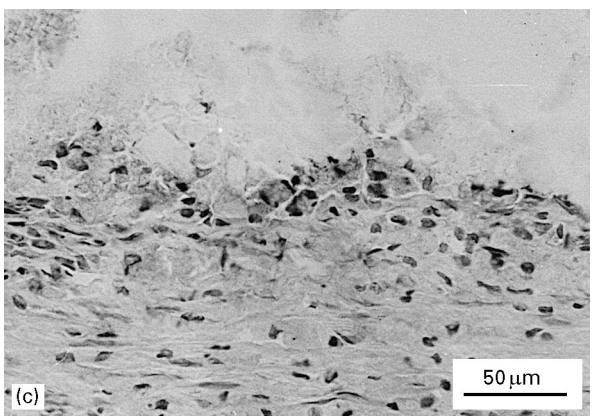

Figure 1 Light microscopy views of the connective tissue capsule surrounding the PLA implant (Haematoxylin–eosin staining). (a) At week 12, a few inflammatory cells are still detected. (b) At week 36, low-grade inflammation has disappeared and the PLA implant is surrounded by collagen fibres and fibroblasts. (c) At week 48 numerous fibroblasts are observed adjacent to the tissue–implant interface, inflammatory cells have diffusely infiltrated connective tissue in most cases observed.

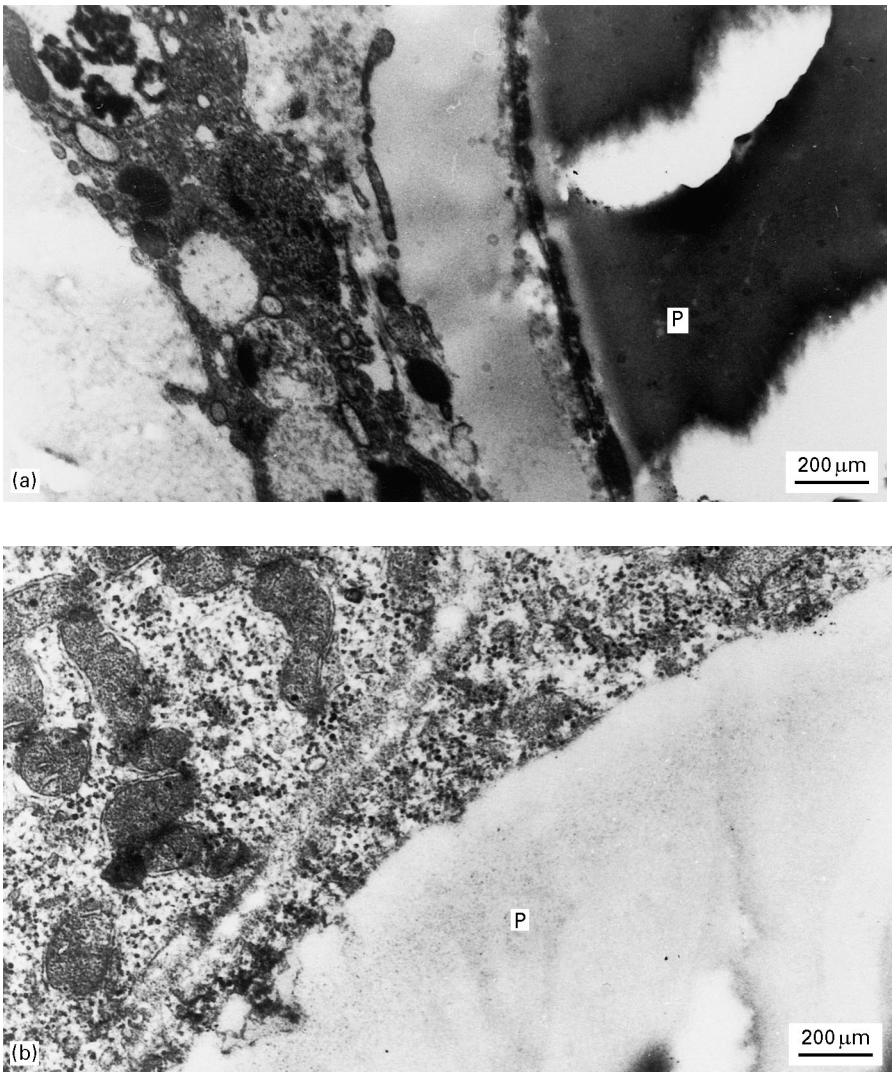

Figure 2 Electron micrographs of connective tissue in close contact with the PLA implant. (a) Between the PLA implant (p) and connective tissue, amorphous substance can be detected, while the cell-to-PLA contact was tight in most cases observed. (b) Numerous mitochondria were seen in the cell close to the PLA implant (p).

TABLE I Characteristic data of the poly-*L*/*D*-lactic acid stereocopolymers with *L*-lactide/*D*-lactide molar ratio of 85/15

	Follow-up (wk)	Tensile strength (e.o./g.i.) (MPa)	M_v(e.o./g.i.) (g mol^{-1})	Mean crystallinity (e.o./g.i.) (%)
In vitro	0	43.8/33.1	61 052/38 484	6.4/12.6
	1	32.9/22.6	54 468/41 170	8.3/10.2
	4	26.1/13.9	45 970/31 320	8.3/13.0
	16	18.9/–	36 497/–	14.9/–
	26	4.1/–	22 730/–	17.1/–
In vivo	0	43.8/33.1	61 052/38 484	6.4/12.6
	4	–/–	51 599/31 320	9.0/14.0
	16	–/–	27 561/12 731	16.7/17.1

33.1 MPa for g.i. implants. Tensile strengths could not be measured *in vivo*, based on the fragility.

Inherent viscosities and crystallinities are shown in Table I. The initial mean molecular weight for e.o. and g.i. implants were subsequently 61 052 and 38 484 g mol^{-1}. During the 16 wk *in vivo* follow-up, molecular weights decreased to 27 561 and 12 731 g mol^{-1}. At the same time, the crystallinity increased from 6.3% to 16.7% (e.o.) and from 12.6% to 17.1% (g.i.).

4. Discussion

The wound healing is characterized by a complex cascade in which intercellular and cell-to-ECM interaction conduct an essential role [10, 18]. Both cFn and Tn have a restricted and transient appearance in healing wound. They are upregulated first at the periphery of the wound and only after a few days are expressed homogeneously throughout the wound ECM, providing a suitable condition for cell movements, deposition and organization of ECM proteins [8, 19]. In normal wound healing, Tn is absent from fibrous components of the scar by 3–4 wk [20].

In our study, an intense immunoreactivity for Tn on implanted PLA was continued 36 wk before

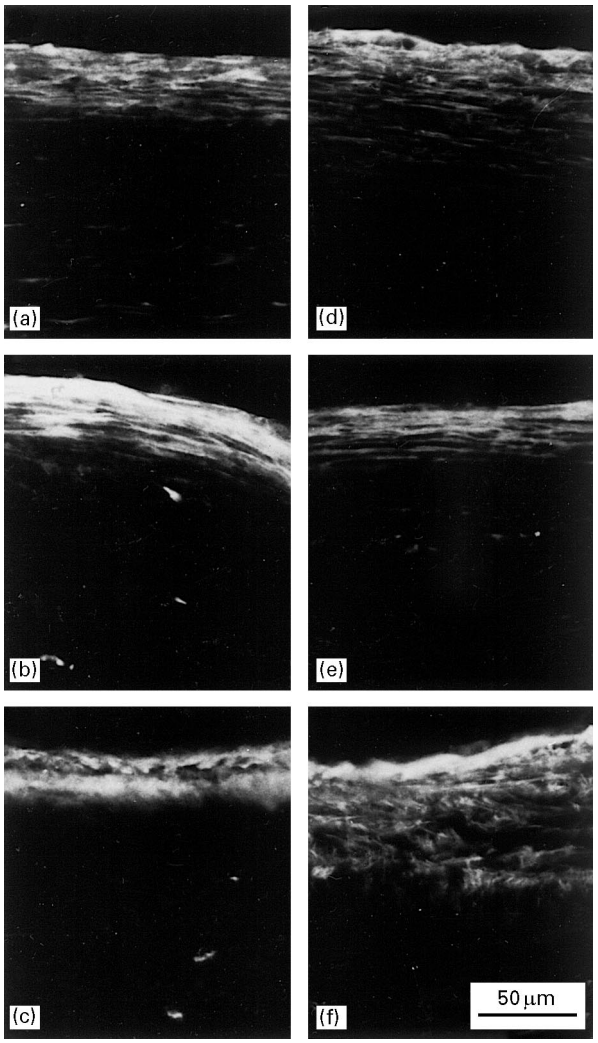

Figure 3 Fluorescence micrographs of tissue adjacent to the PLA implants. (a–c) Stained with MAbs 100EB2 against human Tn, and (d–f) with 52DH1 against human cFn 4, 12 and 36 wk specimens. High Tn and cFn immunoreactivities were detected regularly in close contact with PLA plates.

downregulation, which means a clear prolonged appearance compared with normal wound healing. Earlier studies have demonstrated only transient inflammatory and foreign-body reactions around implanted PLA [21]. Tn influences the synthesis of ECM components, has an immunomodulatory function and, furthermore, has been recently shown to inhibit T-cell activation [22, 23]. Tn has also been suggested to enhance inflammatory reaction in chronic cystitis and cervicitis [24, 25]. High Tn and cFn contents found close to the implants may hence be a sign of prolonged inflammation. In fact, in trauma patients treated by means of titanium, stainless steel or PLA implants, the complication ratio has been reported to be 5%–12%. The symptoms vary between oedema, unexplained pain, obnoxious sensation, exposure of the implant and infection [21, 26]. The high content of Tn found in this study may give rise to the above-mentioned symptoms.

CFn was detected during the whole observation period and only minor quantitative changes were noticed. Bacterial (especially *S. aureus*) capacity to bind Fn is important for their colonization and initiation of infection [27]. CFn is able to attach to the surface of the substrate, thus facilitating cell anchorage and adhesion [28]. Based on this, bacteria may migrate and adhere to the cFn-coated implant and predispose to bacterial infection.

In this study, the cellularity in the interface region adjacent to PLA implant varied considerably, but the α-actin-rich myofibroblasts seemed to form the dominating cell type, particularly at the end of the study. This is in agreement with other studies. Welch *et al.* [11] and Lossing and Hansson [29] postulated that smooth muscle α-actin-rich myofibroblasts may exert strong contractile forces in the implant capsule. It has also been shown that Tn has a close spatial relationship to α-actin-rich myofibroblasts in non-muscular mesenchyme, proposing that Tn may work as an adhesion molecule in contractile mesenchyme [30]. In this study, the PLA implant started to hydrolyse

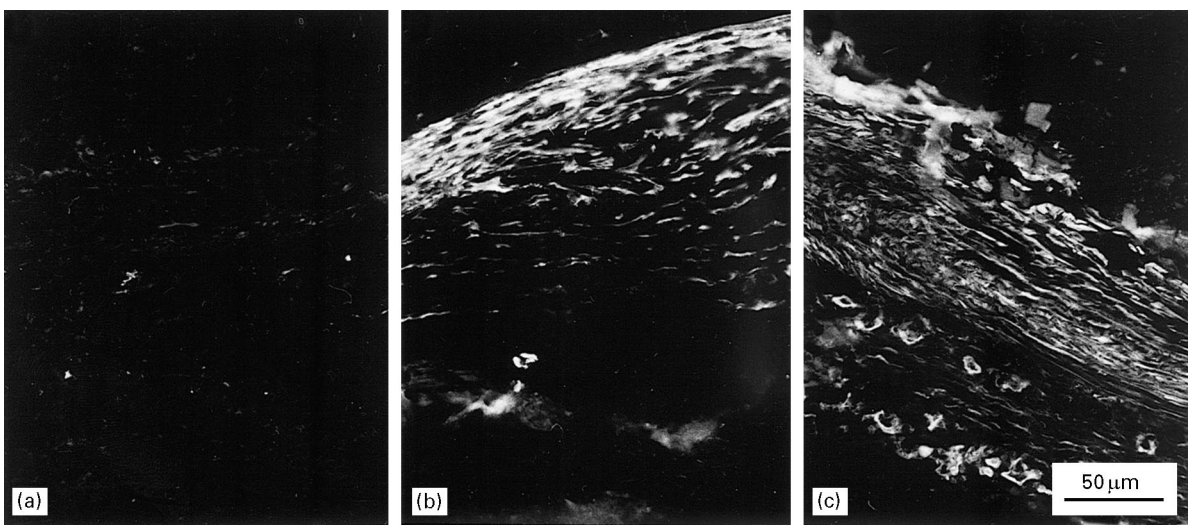

Figure 4 Indirect immunofluorescence micrographs of tissue surrounding the PLA implants at week 48, immunostained (a) for human Tn, (b) EDA-cFn and (c) smooth muscle α-actin. Immunoreaction for Tn is not detected on the 48 wk specimen while that for cFn and α-actin still persisted.

between weeks 36 and 48. At this stage the connective tissue contracts, which was also reflected by the rich myofibroblast content adjacent to the implant. It was notable, however, that Tn was no longer detected on 48 wk specimens while myofibroblasts were still present. While the expression of Tn was downregulated, cFn expression continued. This suggests that cFn, rather than Tn, might be involved in α-actin-mediated contraction. This is in agreement with the published article by Grinnell [31], but deviates from data published by Murakami *et al.* [30].

Ethylene oxide sterilization has been claimed harmful due to potential residues left in implants. Foreign-body reaction with polyglycolide implants has been connected, at least in part, with ethylene oxide [32]. In the present study, we found no differences in tissue responses between gamma irradiation and ethylene oxide sterilization.

Due to processing and sterilization, inherent viscosity of raw material decreased almost to one-third and continued to decrease substantially during implantation *in vivo*. Because of the intense decrease of tensile strengths *in vivo* in both e.o. and g.i. plates, tensile strengths could not be studied. Crystallinity increased steadily to 17.3% (g.i.) and to 16.7% (e.o.). The increase in crystallinity was probably due to preferential cleavage of D-unit containing sequences and increased the mobility of the degraded chains which allowed them to undergo cold crystallization. Semi-crystalline polylactides made amorphous by the rapid cooling process has been reported to crystallize while degrading in other studies, too [16].

It seems that studied poly-*L*/*D*-lactic acid stereocopolymer plate form implants (molar ratio of 85/15) cannot be used for fracture fixation.

5. Conclusions

A prolonged and enhanced expression of both Tn and cFn in connective tissue adjacent to the implanted PLA was detected in this study. Both Tn and cFn play an important role in cell-to-ECM interactions. These proteins participate differently in chronic inflammation and wound healing. Tn, cFn and myofibroblasts are active factors in wound contraction, in healing wounds. Tn has a restricted distribution and is downregulated when maturation has taken place. In this study, at 48 wk, hydrolysation of PLA implants continued, moderate upregulation of myofibroblasts was seen and a profound Tn downregulation was detected before wound healing had ended.

Although Tn expression was decreased to the end of the study, its temporal expression was clearly longer than in normally healing wound. Thus it seems logical to assess that implanted PLA is detected by cells, which, in turn, release Tn and cFn. The reason why Tn was downregulated before cFn at this particular healing stage remains obscure.

While there is much controversy of Tn and cFn function during wound healing, it has been concluded that both are needed for contraction. In the present study, on 48 wk specimens, Tn was no longer detected, although wound contraction was continuing. Our results suggest that Tn is no a major factor in wound contraction. The data shown in this study provide information of interaction between implanted biodegradable material and adjacent connective tissue. The high and prolonged Tn and cFn expression found in this study may partly explain inflammation around PLA implants.

Acknowledgements

Skillful technical assistance of Ms Paula Hasenson, Mr Reijo Karppinen and Mr Hannu Kamppinen is acknowledged. This study was supported by grants from the Finnish Medical Faculty and from the Finnish Dental Society.

References

1. O. BÖSTMAN, S. VAINIONPÄÄ, E. HIRVENSALO, A. MÄKELÄ, K. VIHTONEN, P. TÖRMÄLÄ and P. ROKKANEN, *J. Bone Joint Surg.* (*Br.*) **69** (1987) 615.
2. P. ROKKANEN, O. BÖSTMAN, S. VAINIONPÄÄ, K. VIHTONEN, P. TÖRMÄLA, J. LAIHO, J. KILPIKARI and M. TAMMINMÄKI, *The Lancet* **1** (1985) 1422.
3. O. BÖSTMAN, E. PARTIO, E. HIRVENSALO and P. ROKKANEN, *Acta Orthop. Scand.* **63** (1992) 173.
4. S. SANTAVIRTA, Y. T. KONTTINEN, T. SAITO, M. GRÖNBLAD, E. PARTIO, P. KEMPPINEN and P. ROKKANEN, *J. Bone Joint Surg.* (*Br.*) **72B** (1990) 597.
5. E. J. BERGSMA, F. R. ROZEMA, R. R. M. BOS and W. C. DEBRUIJN, *J. Oral Maxillofac. Surg.* **51** (1993) 666.
6. J. KOVACSJ and L. DEPIETRO, *FASEB J.* **8** (1994) 854.
7. R. CHIQUET-EHRISMANN, E. J. MACKIE, C. A. PEARSON and T. SAKAKURA, *Cell* **47** (1986) 131.
8. V. E. GOULD, V. MARTINEZ-LACABE, I. VIRTANEN, K. M. SAHLIN and M. M. SCHWARTZ, *Lab. Invest.* **67** (1992) 71.
9. M. LUOMANEN and I. VIRTANEN, *J. Oral Pathol. Med.* **21** (1992) 1.
10. R. RAGHOW, *FASEB J.* **8** (1994) 823.
11. M. P. WELCH, G. F. ODLAND and R. A. F. CLARK, *J. Cell. Biol.* **110** (1990) 133.
12. R. CHIQUET-EHRISMANN, *FASEB J.* **4** (1990) 598.
13. A. A. HOWEEDY, I. VIRTANEN, L. LAITINEN, N. S. GOULD, G. K. KOUKOULIS and V. E. GOULD, *Lab. Invest.* **63** (1990) 798.
14. T. VARTIO, L. LAITINEN, O. NÄRVÄNEN, M. CUTOLO, L. E. THORNELL, L. ZARDI and I. VIRTANEN, *J. Cell. Sci.* **88** (1987) 419.
15. E. W. FISCHER, H. J. STERZEL, G. WEGNER, *Koll. Z. Z. Polym.* **251** (1973) 980.
16. H. PISTNER, D. R. BENDIX, J. MUHLING and J. F. REUTHER, *Biomaterials* **14** (1993) 291.
17. S. GOGOLEWSKI, M. JOVANOVIC, S. M. PERREN, J. G. DILLON and M. K. HUGHES, *J. Biomed. Mater. Res.* **27** (1993) 1135.
18. V. LIGHTNER, *J. Invest. Dermatol.* **3** (1994) 273.
19. P. BETZ, A. NERLICH, J. TUBEL, R. PENNING and W. EISENMENGER, *Int. J. Legal Med.* **105** (1993) 325.
20. E. J. MACKIE, W. HALFTER and D. LIVERANI, *J. Cell. Biol.* **107** (1988) 2757.
21. O. M. BÖSTMAN, H. K. PIMLAJAMÄKI, E. PARTIO and P. U. ROKKANEN, *Clin. Orthop.* **320** (1995) 101.
22. T. J. HEMESATH, L. S. MARTON and K. STEFANSSON, *J. Immunol.* **152** (1994) 5199.
23. C. R. RUEGG, R. CHIQUET-EHRISMANN and S. S. ALKAN, *Proc. Nat. Acad. Sci.* **86** (1989) 7437.

24. O. TIITTA, T. WAHLSTRÖM, J. PAAVONEN, A. LANNALA, S. SHARMA, V. E. GOULD and I. VIRTANEN, *Am. J. Pathol.* **141** (1992) 907.
25. O. TIITTA, T. WAHLSTRÖM, I. VIRTANEN and V. E. GOULD, *Wircows Arciv. B Cell Pathol.* **63** (1993) 283.
26. T. J. FRANCEL, B. C. BIRELY, P. R. RINGELMAN and P. N. MANSON, *Plast. Reconstr. Surg.* **90** (1992) 568.
27. T. PÄÄLLYSAHO, K. TERVO, T. KIVELÄ, I. VIRTANEN. A. TARKKANEN and T. TERVO, *Graefe's Arch. Clin. Exp. Opthalmol.* **231** (1993) 61.
28. F. B. BAGAMBISA, H. F. KAPPERT and W. SCHILLI, *J. Oral Maxillfac. Surg.* **52** (1994) 52.
29. C. LOSSING and H-A. HANSSON, *Plast. Reconstr. Surg.* **7** (1993) 1277.
30. R. MURAKAMI, I. YAMAOKA and T. SAKAKURA, *Int. J. Biol.* **33** (1989) 439.
31. F. GRINNELL, *J. Cell Biol.* **4** (1994) 401.
32. P. J. LANDRIGAN, T. J. MEINHARDT, J. GORDON, J. A. LIPSCOMB. J. R. BURG, L. F. MAZZUCKELLI, T. R. LEWIS, T. R. LEWIS and R. A. LEMEN, *Am. J. Ind. Med.* **6** (1984) 103.

Received 27 January
and accepted 25 September 1997